Insulin Receptor Autophosphorylation. II. Determination of Autophosphorylation Sites by Chemical Sequence Analysis and Identification of the Juxtamembrane Sites†

R. A. Kohanski

Department of Biochemistry, The Mount Sinai School of Medicine, 1 Gustave L. Levy Place, New York, New York 10029

Received October 6, 1992; Revised Manuscript Received March 12, 1993

ABSTRACT: Autophosphorylation sites of the human insulin receptor were identified by microsequence analysis of 19 discrete tryptic [^{32}P]phosphopeptides, purified from the autophosphorylated cytoplasmic kinase domain (CKD). Seventeen phosphopeptides were generated by cleavage at Arg and/or Lys, but two phosphopeptides were generated reproducibly by anomalous cleavages. Two new sites were identified in the juxtamembrane region of the intact insulin receptor β-subunit (the amino terminus of the CKD), including phosphotyrosines 965 and 972. Three sites in the central region, including phosphotyrosines 1158, 1162, and 1163, were identified from six phosphopeptides; tyrosine at 1158 was the least phosphorylated. Monophosphopeptides contained phosphotyrosine at either residue 1158 or 1163, but not at 1162. Bisphosphorylation included phosphotyrosines only at 1162 and 1163. The two autophosphorylation sites near the carboxy terminus were found in seven phosphopeptides, including phosphotyrosines at 1328 and 1334. When mapped by reverse-phase high-performance liquid chromatography, these phosphopeptides eluted in the order central domain, first; carboxy-terminal region, second; and juxtamembrane (amino-terminal) domain, last.

The insulin receptor is a hormonally regulated protein(tyrosine) kinase, first reported by Kasuga et al. (1983a,b). The intracellular kinase activity of this receptor's transmembrane β-subunit is stimulated by insulin binding to the extracellular α-subunit. In addition, autophosphoryaltion can be stimulated by polycations (Morrison et al., 1989; Biener & Zick, 1990; Fujita-Yamaguchi et al., 1989; Sacks & McDonald, 1988; Kohanski, 1989) and certain polypeptides derived from the high-affinity substrate RCAM-lysozyme (Kohanski & Schenker, 1991). For the native insulin receptor, similar tryptic [^{32}P]phosphopeptide maps resulted from these stimulated states, whether induced by insulin, polycations, or the polypeptides (Kohanski, 1989; Kohanski & Schenker, 1991). In the preceding paper in this issue (Kohanski, 1993), phosphopeptide mapping was used to show that the purified cytoplasmic kinase domain autophosphorylation mimics that of the insulin receptor in the absence of insulin. It was also shown that the distribution of autophosphorylation sites was sensitive not only to insulin, for the native receptor, but also to the concentration of ATP for both forms of the enzyme. In order to interpret these tryptic [^{32}P]phosphopeptide maps, it was necessary to identify the specific sites of autophosphorylation represented by each peak of radioactivity in the map.

To accomplish this goal, we utilized the cytoplasmic kinase domain (CKD)[1] of the human insulin receptor subcloned into baculovirus by homologous recombination and expressed in Sf9 cells (Villalba et al., 1989). The purification of milligram amounts of this form of the enzyme permitted direct chemical sequence analysis of the tryptic [^{32}P]phosphopeptides derived from the CKD. Although five of the possible 13 autophosphorylation sites have been identified previously in the central and C-terminal subdomains of the enzyme, the juxtamembrane subdomain site(s) remain unassigned (Herrera & Rosen, 1986; White et al., 1988; Flores-Riveros et al., 1989; Tornqvist et al., 1987; Tavare & Denton, 1988). In this study, we have purified and sequenced mono-, bis-, and trisphosphorylated [^{32}P]phosphopeptides from the ^{32}P-labeled CKD. These results established the subdomains from which each phosphopeptide originated and the identities of each phosphotyrosine, including the two tyrosyl groups of the juxtamembrane domain that undergo autophosphorylation.

EXPERIMENTAL PROCEDURES

Materials. [^{32}P]Orthophosphate was obtained from ICN Radiochemicals. [γ-^{32}P]ATP was synthesized according to the method of Walseth and Johnson (1979) and purified (Palmer & Avruch, 1981). HEPES,[1] DTT, ATP, and electrophoresis reagents were from Boehringer/Mannheim Biochemicals. Trypsin was from Worthington (*N*-tosyl-L-phenylalanine chloromthyl ketone treated) or from Boehringer/Mannheim. Chromatography reagents were HPLC grade. Matrices and high-pressure columns are mentioned in the text. The intact 48-kDa cytoplasmic kinase domain (CKD) of the human insulin receptor was expressed in Sf9 cells and purified, essentially as described by Villalba et al. (1989). Cell culture reagents were from Gibco. The recombinant baculovirus containing CDNA for the CKD was a gift of the late Dr. Ora Rosen.

Autophosphorylation of the Cytoplasmic Kinase Domain. The preparative scale autophosphorylation reactions were each done in a volume of 500 μL, containing 11 μM CKD, 500 μM [γ-^{32}P]ATP, 5 mM $Mn(CH_3CO_2)_2$, 50 mM HEPES, and 1 mM DTT, at pH 7.0. Additional reactions were done at 1.1 μM CKD and 50 μM [γ-^{32}P]ATP and 20 μM [γ-^{32}P]ATP. A single specific activity was used for all the reactions, at $\geq$7000 cpm/pmol, measured by Cherenkov counting (i.e.,

† Supported by Grant DK 38893 from the National Institutes of Health.

[1] Abbreviations: CKD, cytoplasmic kinase domain of the human insulin receptor; DTT, dithiothreitol; HEPES, 4-(2-hydroxyethyl-1-piperazine)ethanesulfonic acid; HPLC, high-performance liquid chromatography; PTH-Tyr, *N*-phenylthiohydantion derivative of tyrosine; SDS–PAGE, sodium dodecyl sulfate–polyacrylamide gel electrophoresis; TFA, trifluoracetic acid; Tris, tris(hydroxymethyl)aminomethane.

0006-2960/93/0432-5773$04.00/0

without scintillant in the ^{14}C channel of the liquid scintillation counter). The reactions were carried out at room temperature for 60 min and quenched by the addition of 200 μL of 40% trichloroacetic acid in water (w/v). The mixtures were held in an ice bath for 20 min, and then the precipitated protein was collected by centrifugation. The pellets were washed twice with 1 mL of ether and allowed to air dry. The precipitates were dissolved in 35 μL of 3-fold concentrated sample buffer and diluted with 70 μL of water, and the ^{32}P-labeled CKD was isolated by SDS–PAGE (see below).

Analytical scale autophosphorylations were performed at 0.25 μM or 0.15 μM CKD, using either the intact 48-kDa form or the 38-kDa form derived by partial proteolysis with immobilized trypsin (Boehringer/Mannheim) followed by gel permeation chromatography. The final concentration of [γ-^{32}P]ATP was 100 μM, and all other reactants were at the final concentrations given above. The reaction volume was 50 μL. The reaction was quenched by the addition of concentrated sample buffer, and the products were resolved by SDS–PAGE.

Sodium Dodecyl Sulfate–Polyacrylamide Gel Electrophoresis. To isolate the ^{32}P-labeled CKD, we used the following conditions for SDS–PAGE. The protocol of Laemmli (1970) was used with modifications. The composition of the gels and the running conditions affect the results of these experiments and are therefore given in detail. The acrylamide was stored over AG1-X8 anion exchange resin (1 g of resin per 50 mL of stock 50% acrylamide solution); this solution was stored at 4 °C and used within 2 weeks for these experiments. A fresh stock solution of 1% ammonium persulfate (w/v in water) was used immediately. The buffers for the separating and stacking gels were prepared as 5- and 10-fold concentrated stocks, respectively, and were sterile filtered before storage at 4 °C. The separating gel composition was 12.5% T (2.5% C), 0.375 M Tris (pH 8.8), 0.1% SDS (w/v), 0.025% ammonium persulfate (w/v), and 0.05% TEMED (v/v). The stacking gel composition was 5% T (2.5% C), 0.125 M Tris (pH 6.7), 0.1% SDS (w/v), 0.05% ammonium persulfate (w/v), and 0.1% TEMED. Each solution was degassed before the addition of SDS or TEMED. The polymerized gels were allowed to stand at room temperature for 24 h before use. The gels were run at constant voltage (80 V, 2.5 h) at room temperature, using the Tris–glycine buffer of Laemmli (1970). The apparatus was the Bio-Rad minicell, using 1.5-mm thick gels and 10-well sample combs.

Digestion with Trypsin. The ^{32}P-labeled CKD was located by autoradiography from the wet, unfixed gel, immediately after electrophoresis. These segments were excised from the gels and soaked in 35 mL of water for 30 min, and the water was exchanged once. Each segment was then crushed in a 1.5-mL conical microcentrifuge tube. Trypsin, at a concentration of 0.1 mg/mL, was then added in 1 mL of 50 mM *N*-ethylmorpholine acetic acid, pH 8.7. The crushed gel pieces were kept suspended by rocking the sealed tubes for 16 h, at room temperature. The solution containing the tryptic fragments was separated from the gel pieces by filtration in Millipore Ultrafree centrifugal filtration units (0.2-μm pore membranes) and lyophilized in a Savant SpeedVac. The same results were achieved using trypsin from either Worthington or Boehringer/Mannheim.

Purification of [^{32}P]Phosphopeptides. The chromatograph was a Hewlett Packard model 1090, equipped with automated sample injection, and also fitted in the lab with a Rheodyne manual injector with a 2-mL sample loop. Detection was done with a Linear Instruments model 206PHD UV/Vis detector with a 10-mm path length, 15-μL flow cell, or a Radiomatic Flo-One Beta continuous flow radiation detector fitted with a 120-μL flow cell rebuilt in the laboratory to minimize the volumes of the inlet and outlet tubing. Data were collected by computer. Fractions were collected on a time program using a Gilson Model 201 fraction collector.

Samples comprising 5% of each digest were reserved for analytical separations by HPLC. The [^{32}P]phosphopeptides were purified from the remaining 95% of each digest. The lyophilized digests from the preparative scale reactions at 20, 50, and 500 μM [γ-^{32}P]ATP were pooled and dissolved in 200 μL of 20 mM $NH_4CH_3CO_2$, pH 6.0, and 195 μL was injected onto a 2.1 × 250 mm SynChropak AX300 weak anion exchange column, using the automated sample injector; the manual injection valve was not in-line. The buffers used were (A) 20 mM $NH_4CH_3CO_2$, pH 6.0; and (B) 1 M KH_2PO_4, pH 4.0. The flow rate was 0.6 mL/min, and fractions of 1 min each were collected. The elution gradient was 0–80 min, a linear increase from 0 to 30% B, and 80–150 min, a linear increase from 30 to 100 %B. Fractions were pooled according to the distribution of radioactivity, as described under Results.

Samples from each pool were reserved for analytical chromatography. The remaining 95% of each pool was applied to a 2 × 150 mm Spherisorb C8 reverse-phase column, using the 2-mL sample loop. During this loading procedure, the effluent was monitored for breakthrough of radioactivity with the Radiomatic detector. Since the breakthrough was generally less than 5% of the applied sample, it was discarded. However, to minimize the breakthrough, it was essential that the column was equilibrated in 0.15% TFA in water (w/v) for 1 h at a flow rate of 0.25 mL/min before loading the sample. The 2-mL sample loop was not in-line during the elution, and the effluent was directed to the Linear 206PHD UV/Vis detector instead of the Radiomatic Flo-One Beta. The [^{32}P]phosphopeptides were eluted using the following gradient (solvent A = 0.15% TFA in water, w/v, and solvent B = 0.15% TFA in acetonitrile, w/v): 0–2 min, a linear increase of 0–8% B; 2–25 min, isocratic at 8% B; 25–115 min, a linear increase of 8–32.5% B. The flow rate was constant at 0.25 mL/min. Fractions were monitored for radioactivity by Cherenkov counting and were pooled according to the presence of radioactivity and by inspection of the chromatograms at 215 nm, as described under Results. Pooled [^{32}P]phosphopeptides were lyophilized and stored dry at −20 °C until sequence analysis.

Sequence Analysis of [^{32}P]Phosphopeptides. The amount of each [^{32}P]phosphopeptide taken for sequence analysis was typically 25–40 pmol, based upon the specific activity of the [γ-^{32}P]ATP as the only quantitative measure prior to sequencing. In several cases, all of the purified [^{32}P]phosphopeptide was taken for a single attempt at sequencing since there was ≤20 pmol of [^{32}P]phosphopeptide, based upon the specific activity. Analyses were performed on a Porton Instruments model 2090 gas phase sequencer using on-line PTH-amino acid identification, with 4% triethylamine in water as the base, and the software supplied by the manufacturer. PTH-amino acid standards were from Pierce Chemical Co. PTH-phosphotyrosine was not recovered in sufficient quantities to be detected with the single wavelength (269 nm) employed on the chromatograph, but the analinothiozolinone–phosphotyrosine, eluting as a broad peak at ≈10 min, was detected for some [^{32}P]phosphopeptides using the Radiomatic Flo-One Beta detector to monitor the column effluent for each sequencer cycle, as discussed under Results. Each [^{32}P]phosphopeptide was dissolved in 0.15% TFA (w/v) in

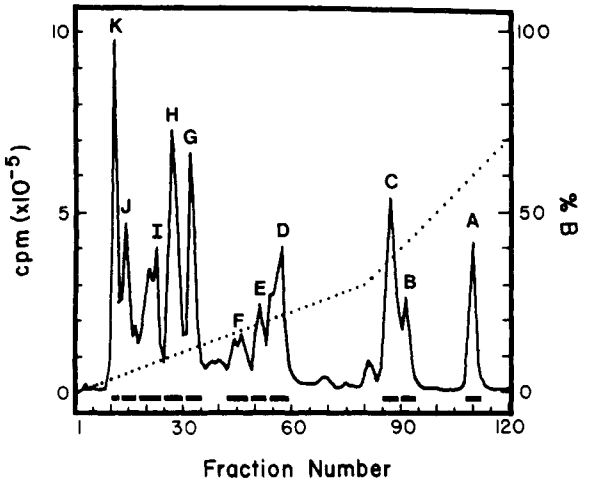

FIGURE 1: High-performance anion exchange chromatography of tryptic [^{32}P]phosphopeptides from the cytoplasmic kinase domain. Autophosphorylation, using 5.5 nmol of 48-kDa CKD, and tryptic digestion were perfomed as described under Experimental Procedures. The initial separation of [^{32}P]phosphopeptides was done on a 2.1 × 250 mm SynChropak AX300 weak anion exchange column. The buffers used were A = 20 mM $NH_4CH_3CO_2$, pH 6.0, and B = 1 M KH_2PO_4, pH 4.0. The flow rate was 0.6 mL/min, and fractions of 1 min each were collected. The elution gradient is indicated by the dotted line, shown as percent B on the right-hand axis, and radioactivity in each fraction was measured in a scintillation counter, without scintillant (left-hand axis). Fractions were pooled according to the distribution of radioactivity, as indicated by the solid bars underneath the elution profile and by the letters above the peaks.

10% acetonitrile (v/v) to give ≈2–5 pmol/μL and applied in aliquots of ≤10 μL each to a peptide support disk supplied by Porton Instruments.

RESULTS

Purification of [^{32}P]Phosphopeptides and Phosphopeptide Nomenclature. The autophosphorylated cytoplasmic kinase domain was used to generate tryptic [^{32}P]phosphopeptides because it could be obtained in greater mass than the purified holomeric insulin receptor. It has been demonstrated that the phosphopeptides generated from both forms of the enzyme are essentially the same (Kohanski, 1993; Tavare et al., 1991; Herrera et al., 1988). Three preparative scale reactions were done at 20, 50, and 500 μM [γ-^{32}P]ATP at a single specific radioactivity, and the tryptic digests from these reactions were pooled for purification.

A two-step protocol was used for the purification. The phosphopeptides were separated initially by anion exchange HPLC, and fractions were pooled according to radioactivity (Figure 1). Aliquots from each pool were then analyzed for the [^{32}P]phosphopeptides present by comparison with the the reverse-phase HPLC profile obtained from the unfractionated digest (Figure 2A). [^{32}P]Phosphopeptides from a given anion exchange HPLC pool are indicated by the letter of that pool and by a number corresponding to the order in which they eluted in the analytical HPLC chromatograms (Figure 2B–J).

Pool A did not contain any [^{32}P]phosphopeptides and may represent residual [γ-^{32}P]ATP present in the gel segments. Pool K contained two [^{32}P]phosphopeptides eluting at 60–63.5 min (eluting just before peak J-3 in Figure 2A), but the majority of the radioactivity in this pool was not adsorbed on the reverse-phase column and remains unidentified. The two peptides were not recovered in sufficient yield to warrant further analysis and in the overall phosphopeptide map were never more than 2% of the total radioactivity present in

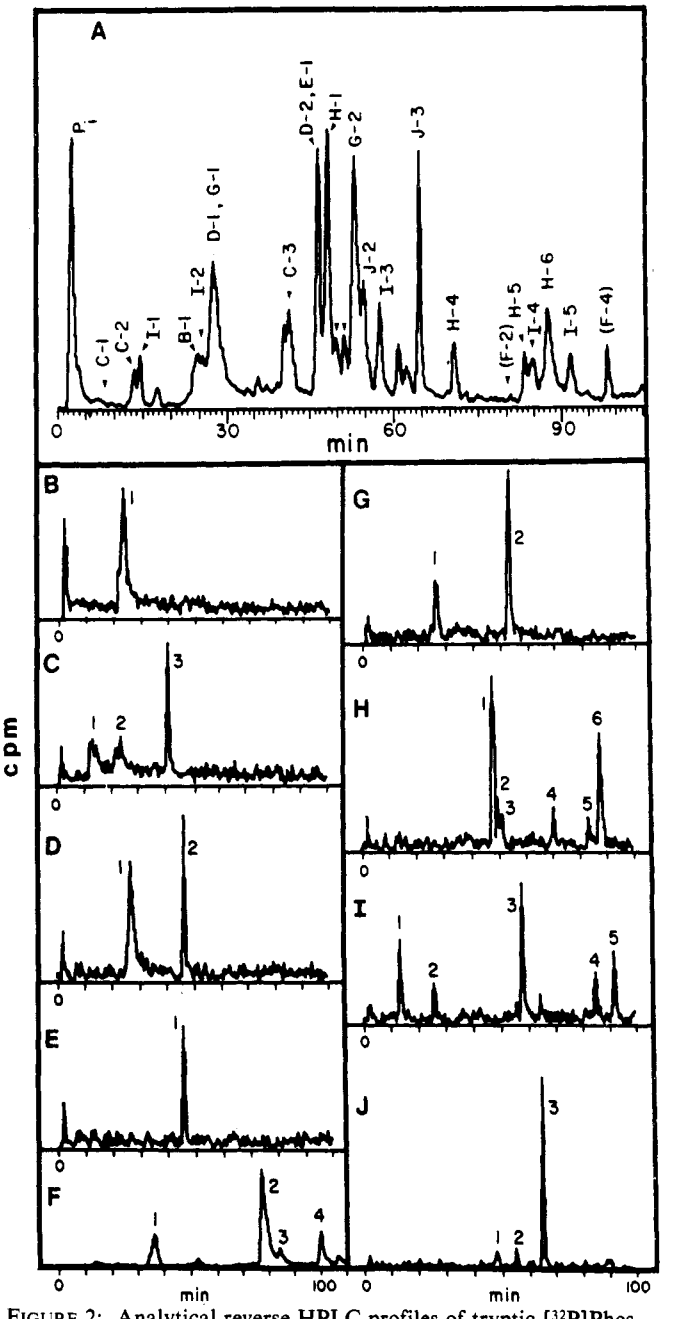

FIGURE 2: Analytical reverse HPLC profiles of tryptic [^{32}P]Phosphopeptides. [^{32}P]Phosphopeptide maps of the complete tryptic digest of autophosphorylated CKD and of the pools obtained from anion exchange HPLC shown in Figure 1. (Panel A) An aliquot of the original tryptic digest from 5.5 nmol of autophosphorylated 48-kDa CKD was mapped to show the rentention times of the phosphopeptides in the mixture. (Panels B–J) Analytical separations of phosphopeptides pooled from anion exchange HPLC; each panel corresponds to the anion exchange pool designated in Figure 1. The [^{32}P]phosphopeptides were numbered in the order of elution, and their retention times were used to make the designations shown in panel A. The phosphopeptides shown in panels C and F were from a separate autophosphorylation reaction, tryptic cleavage, and anion exchange HPLC isolation. Further details are given under Results.

analytical maps. The remaining anion exchange pools each contained phosphopeptides (Figure 2, panels B–J). Pools B and E each contained a single phosphopeptide. Pools D and G each contained two phosphopeptides, and the remaining pools were more complex. The coelution of phosphopeptides D-1 and G-1 were confirmed by mixing these phosphopeptides and repeating the analytical chromatogram, similarly for the coelution of phosphopeptides D-2 and E-1. The assignments for phosphopeptides B-1, C-1, C-3, I-1, I-2, and J-2 were

Table I: Central Domain Phosphopeptides[a]

	number and sequence[b]								
PPEP	Asp	Ile	1158 Tyr	Glu	Thr	Asp	1162 Tyr	1163 Tyr	Arg
B-1	8.6	5.0	6.5	10.1	7.4	7.3	(P)	(P)	(R)
C-1	9.6	7.5	(P)	7.8	6.1	6.1	(P)	(P)	(RK)
C-3	10.3	5.7	6.0	7.1	5.3	6.6	(P)	(P)	(RK)
D-1	9.7	5.1	5.0	6.8	4.3	7.1	(P)	(P)	(RKGGK)
D-2	22.5	13.8	15.7	17.1	13.1	12.8	4.1	(P)	(R)
E-1	26.3	17.4	(P)	19.4	8.2	15.7	11.8	16.4	3.3

[a] Sequence analysis results are shown for purified phosphopeptides encompassing the central autophosphorylation sites at Tyr^{1151}18, Tyr^{1162}, and Tyr^{1163} [numbered according to Ebina et al. (1985)]. The designations of the phospholipids, purified by anion exchange and reverse-phase HPLC, are given in Figure 2. Phosphotyrosine is indicated as (P). Additional details and the sequence assignments at the carboxy terminus of each peptide are discussed in the text. [b] Values are in picomoles.

made by remixing each phosphopeptide with an aliquot of the complete digest and repeating the analyses.

For sequence analysis, each anion exchange pool was loaded *in toto* onto the same reverse-phase column, and [^{32}P]phosphopeptides were eluted using the same gradient. The effluent was monitored for absorbance from 210 to 300 nm (5-nm intervals) to establish the presence of peptides, and the collected fractions were monitored for radioactivity to determine which were radiolabeled.

There are three clusters of autophosphorylation sites, as reported by others (Herrera & Rosen, 1986; White et al., 1988; Flores Riveros et al., 1989; Tornqvist et al., 1987; Tavare & Denton, 1988): a central domain with three tyrosines, a carboxy-terminal domain with two tyrosines, and a juxtamembrane (amino-terminal) domain with three tyrosines. No other tyrosines from other regions of the cytoplasmic kinase domain appear to react during autophosphorylation. In describing the autophosphorylation sites of the insulin receptor, we will use the numbering of Ebina et al. (1985).

Central Domain Autophosphorylation Sites. This domain includes autophosphorylation sites Tyr^{1158}, Tyr^{1162}, and Tyr^{1163}, corresponding to positions 3, 7, and 8 in the sequence analysis (Table I). Because we made chemical identifications of the PTH-amino acids at each cycle of the Edman degradation, we established directly the presence of tyrosine residues that were *not phosphorylated.* Thus, phosphopeptides D-2 and E-1 were shown to be monophosphoeptides because PTH-Tyr was established at positions two and seven of D-2, and at positions seven and eight of E-1.

By monitoring the effluent from the HPLC connected on-line to the sequencer, we were able to detect ^{32}P if it was released during the first three cycles, but not later. Thus, we detected ^{32}P released in cycle 3 in the analysis of C-1 and E-1, but not for the other phosphopeptides listed in Table I. The ^{32}P liberated and detected was on the order of 2–5% of the applied radioactivity, and, after completing the sequence analysis, ≈75–85% of the radioactivity remained bound to the support filter. This was observed using the Porton Instruments peptide support filter, as well as the arylamine covalent attachment supports from Milligen. We therefore inferred the positions of the phosphotyrosines from the absence of PTH-tyrosine in sequencer cycles where it should have been detected but was not found. In addition, the stoichiometry of peptide phosphorylation was also determined from the ratio of picomoles ^{32}P used for sequence analysis *versus* the picomoles initial yield of the PTH-amino acids, as described below.

By this approach, bisphosphorylation yielding phospho-Tyr^{1162} and phospho-Tyr^{1163} was demonstrated in three peptides shown in Table I. The only trisphosphopeptide was C-1. Thus, the doubly phosphorylated forms in the central domain included phospho-Tyr^{1162} and phospho-Tyr^{1163} but did not include phospho-Tyr^{1158}. To account for three different bisphosphopeptides with the same amino terminus, we assumed that there was carboxy-terminal heterogeneity. This would be due to the sequence Arg-Lys-Gly-Gly-Lys following Tyr^{1163}, giving three tryptic cleavage sites. The probable assignments were based on the order of elution from the anion exchange column (Figure 1).

In summary, six [^{32}P]phosphopeptides were purified and sequenced from the central domain of the CKD. Three were bisphosphopeptides including phospho-Tyr^{1162} and phospho-Tyr^{1163}, two were singly phosphorylated at either Tyr^{1158} or Tyr^{1163}, and one phosphopeptide was triply phosphorylated. The order of elution from the reverse-phase column was consistent with increasing numbers of phosphates promoting earlier elution, as in the cases of D-2 *versus* B-1, and D1 *versus* C1 (Table I and Figure 2).

Carboxy-Terminal Autophosphorylation Sites. This domain includes the autophosphorylation sites Tyr^{1328} and Tyr^{1334}. In principle, there are three likely phosphopeptides: two monophosphopeptides and one bisphosphopeptide. However, the borders of these peptides include Lys-Arg and Lys-Lys sequences at the amino and carboxy termini, respectively. This allows four possible cleavage products for each phosphorylation site, for a total of 12 possible tryptic [^{32}P]phosphopeptides, although seven peptides were purified and sequenced from this domain. Tryptic cleavage at the amino-terminal Lys^{1325}-Arg^{1326} bond was demonstrated for two of these (Table II, I-3 and J-2), and cleavage at Arg^{1326}-Ser^{1327} was demonstrated in the other five phosphopeptides (Table II).

We believe that sequence analysis of these phosphopeptides were complicated by the histidinyl residues. Good sequence results were obtained for one monophosphopeptide, J-3, which included phospho-Tyr^{1334} (Table II). However, the yield of PTH-His in cycle-5 was 2.4-fold lower than the yield of PTH-Glu in the preceding cycle. This was also found with the bisphosphopeptide G-2. It seems likely that these histidinyl residues were modified in some fashion, either during the SDS–PAGE or the generation and purification of the [^{32}P]phosphopeptides.[2] The modified histidine may present an undesirable functional group that reduces *cleavage* during the

[2] Preliminary experiments on [^{32}P]phosphopeptide purification and sequencing indicated that artifactual cleavage occurred at His^{1331}, and these are described under Discussion. The conditions used in this study that reduce these artifactual cleavages are given under Experimental Procedures. The conditions that generated more extensive artifactual cleavages were using aged acrylamide solutions (≥2 weeks) without storage over AG1-X8, using the gels within 2 h of polymerization, and running the SDS–PAGE at high voltage, which produced significant ohmic heating.

Table II: Carboxy-Terminal Phosphopeptides[a]

	number and sequence[b]										
PPEP	Arg	Ser	1328 Tyr	Glu	Glu	His	Ile	Pro	1334 Tyr	Thr	His
G-1		7.8	(P)	7.6	6.8						
G-2		14.4	(P)	12.6	14.8	4.0	5.1	3.5	(P)	4.2	3.0
H-1		20.4	(P)	17.7	23.3						
H-3		6.0	(P)	4.8	5.7		1.8				
I-3	5.0	6.2	(P)	4.2	4.5				(P)		
J-2	18.1	12.9	(P)	15.8	18.4						
J-3		23.4	10.4	22.2	23.3	9.8	12.2	8.1	(P)	10.2	6.0

[a] Sequence analysis results of purified [^{32}P]phosphopeptides containing the autophosphorylation sites at Tyr^{1328} and Tyr^{1334}. The designations of the phosphopeptides, purified by anion exchange and reverse-phase HPLC, are given in Figure 2. Phosphotyrosine is indicated as (P). Further details are given in the text. [b] Values are in picomoles.

Table III: Juxtamembrane Phosphopeptides[a]

	number and sequence[b]											
PPEP	Arg	Gln	Pro	Asp	Gly	Pro	Leu	Gly	Pro	Leu	965 Tyr	Ala
F-2[c]		7.3	5.0	7.1	7.3	3.8	4.4	5.0	3.2	4.3	(P)	3.8
H-6		3.3	1.2	3.3	2.9	0.9					(?)	
I-4[d]		3.4	1.7	3.8	2.5	0.9	2.1		1.1		(?)	
I-5	11.5	9.4	5.1	8.9	5.5	3.7	3.6	4.4	2.5	3.1	(P)	2.3

[a] Sequence analysis results of purified phosphopeptides encompassing the juxtamembrane (amino-terminal) autophosphorylation sites at Tyr^{965} and possibly Tyr^{972}. The designations of the phosphopeptides, purified by anion exchange and reverse-phase HPLC, are given in Figure 2. Phosphotyrosine is indicated as (P). Further details are given in the text. [b] Values are in picomoles. [c] The sequence following Ala^{966} was Ser(1.4)-Ser(2.1)-Asn(1.8)-Gly(1.5)-Glu(1.4); each PTH-amino acid is followed by the quantity in parentheses. [d] This peptide was identified as the minor sequence mixed with an apopeptide F-V-M-D-G-G-Y-L-D-T-... (Tyr^{1227}), which "copurified" after anion exchange and reverse-phase HPLC. This apopeptide had an initial yield of 29.2 pmol versus 4 pmol for I-4. Gly(7) and Leu(9) could not be quantified in the sequence of I-4 because of the lag from the major sequence.

Edman degradation, since neither double coupling nor increased cleavage times improved the yields after His^{1331} (data not shown).

However, the possibility that sequence analyses of phosphopeptides G-1, H-1, I-3, and J-2 failed after the second glutamyl residue resulted from artifactual cleavage at His^{1331} must be considered. As will be described under Discussion, we have found evidence for cleavage at this residue. Two findings in this report argue against this occurrence for the latter three phosphopeptides. First, the elution positions of these phosphopeptides were clustered in the same region, consistent with common chemical structures. Second, there was no decline in yield of the second PTH-Glu, which would have been expected if it were the carboxy-terminal amino acid (e.g., Arg^{1164} of peptide E-1, Table I). On the contrary, an increase in the yield of PTH-Glu was observed (peptides G-2 to J-3, Table II), consistent with the normal lag observed during Edman degradations. In the case of phosphopeptide G-1, there was indeed a decrease in the yield of PTH-Glu, and its elution position was abnormal for phosphopeptides derived from the carboxy-terminal domain. The domain assignment for this peptide is therefore certain, but the exact interpretation of the number of phosphotyrosyl groups is not definitive. Given these difficulties, the mono- and bisphosphopeptides of the carboxy-terminal domain were determined as follows: The [^{32}P]phosphopeptide G-2 was shown to contain two phospho-Tyr groups directly from the sequence analysis, since PTH-Tyr was completely absent at all cycles of the analysis (Table II). Phosphopeptide I-3 was determined to be a bisphosphopeptide based upon the input/initial yield ratio:[3] the average ratio for bisphosphopeptides G-2, B-1, C-3, and D-1 was 3.1 ± 0.4, and the ratio was 3.0 for I-3. In accordance with this analysis, discussed in more detail below, phosphopeptides H-1, H-3, and J-2 were determined to be monophosphopeptides, since their input/initial yield ratios were 1.6, 1.8, and 1.5, respectively, compared to an average ratio of 1.6 ± 0.2 for the three monophosphopeptides already sequenced (D-2, E-1, and J-3). Peptide J-3 was shown directly to be a monphosphopeptide.

Juxtamembrane Autophosphorylation Sites. To date, no one has identified the autophosphorylation sites in this domain, which include Tyr^{964}, Tyr^{972}, and Tyr^{984}, and which is also the amino-terminal domain of the CKD. Amino-terminal heterogeneity of these peptides was anticipated, and indeed observed, since the amino terminus of the CKD (the first juxtamembrane residues of the β-subunit) is Arg-Lys-Arg-Gln^{956}, which represent multiple potential tryptic cleavage sites.

Phosphopeptides F-2 and I-5 were both shown to contain phospho-Tyr^{965} by direct sequence analysis, differing by the absence versus the presence of Arg^{955}, respectively (Table III). Despite the input/initial yield ratio of 2.8, phosphopeptide I-5 may not include a second phosphotyrosine because the repetitive yield was compromised by the three prolyl residues. In the case of F-2, we obtained extensive sequence information by using a double-coupling double-cleavage protocol to increase the repetitive yields after the three prolyl residues. However, we could not sequence past the second tyrosyl group, so we could not determine its phosphorylation state. Phosphopeptides H-6 and I-4 were shown conclusively to originate from the juxtamembrane domain. However, the exact phosphorylation sites were not determined, and we could not make a reliable inference about the stoichiometries of phosphorylation because the N-terminal Gln may have partially cyclized.

Finally, we were able to demonstrate a second juxtamembrane phosphorylation site by sequence analysis of phospho-

[3] The input/initial yield ratio is calculated as the picomoles of [^{32}P]phosphopeptide applied to the peptide filter for sequence analysis, determined from the amount of ^{32}P present and the specific activity of the [γ-^{32}P]ATP, compared to the picomoles of initial yield of PTH-amino acids from the sequence analysis.

Table IV: Juxtamembrane Phosphopeptides from Abnormal Cleavages[a]

	number and sequence[b]									
PPEP	Ala	Ser	Ser	Asn	Pro	Glu	972 Tyr	Leu	Ser	Ala
H-4			11.0	6.9	3.1	5.1	(P)	2.5	2.9	3.1
I-1	7.3	9.2	11.9	4.8	3.8		(?)			

[a] Sequence analysis results of purified phosphopeptides encompassing the juxtamembrane autophosphorylation site at Tyr^{972}. The amino-terminal sequences indicate that cleavage at Tyr^{965} and/or at Ser^{967} resulted in the generation of these peptides. The designations of the phosphopeptides, purified by anion exchange and reverse-phase HPLC, are given in Figure 2. Phosphotyrosine is indicated as (P). Further details are given in the text. [b] Values are in picomoles.

Table V: Stoichiometries of [^{32}P]Phosphate per Phosphopeptide[a]

PPEP	input for sequence (pmol ^{32}P)	initial yield (pmol PTH-aa)	ratio	stoichiometry ^{32}P/PPEP (pmol/pmol)
B-1	33	10	3.3	2
C-1	36	7	5.1	3
C-3(*)	31	10	3.1	2
D-1	34	10	3.4	2
D-2(*)	39	23	1.7	1
E-1(*)	40	26	1.5	1
F-2	18	8	2.3	1–2
G-1	21	8	2.6	?
G-2(*)	41	15	2.7	2
H-1	31	20	1.6	1
H-3	11	6	1.8	1
H-4(*)	16	10	1.6	1
H-6	20	4	5.0	?
I-1	19	12	1.6	1
I-3	18	6	3.0	2
I-4	21	4	5.3	?
I-5	33	12	2.8	1–2
J-2	27	18	1.5	1
J-3(*)	34	23	1.5	1

[a] The [^{32}P]phosphopeptides were purified from a tryptic digest of autophosphorylated 48-kDa cytoplasmic kinase domain and sequenced, as described in Tables I–IV. The stoichiometries of [^{32}P]phosphate per phosphopeptide were determined from the ratios of input picomoles measured as ^{32}P in the sequencer versus the initial yield of PTH-amino acids from the sequence analysis; the latter data are found in Tables I–IV. Data from phosphopeptides (PPEP; see Figure 2A) marked with an asterisk (*) were used to standardize this analysis. Further details are given in the text.

peptides H-4 and I-1 (Table IV). Peptide H-4 arose by an anomalous cleavage at Ser^{968}, and I-1 by cleavage at Ala^{966}, both of which cleavages we are at a loss to explain. We conclude that H-4 and I-5 were monophosphopeptides, based upon input/initial yield ratios of 1.6 for both.

In summary, we have now reported the identification of two phosphorylation sites in the amino terminus of the CKD, which correspond to Tyr^{965} and Tyr^{972} in the juxtamembrane region of the native insulin receptor's β-subunit.

Stoichiometries of [^{32}P]Phosphate per Phosphopeptide. The input versus initial yield ratios[3] were used to establish the numbers of phosphotyrosyl groups in many peptides for which sequence information was incomplete. These ratios are summarized in Table V. This approach was standardized from phosphopeptides originating in each of the three domains for which the most complete sequence information was obtained. The results of these sequence analyses are summarized in Figure 3. This scheme shows the multiple phosphopeptides that were purified from each domain of the CKD and that some phosphopeptides arose from unexpected cleavages. It remains unclear if there were bisphosphopeptides originating from the juxtamembrane domain, or if the multiplicity of these phosphopeptides resulted from carboxy-terminal heterogeneity of tryptic cleavage. However, it seems likely that such a bisphosphopeptide was present, since heterogeneous C-terminal cleavage could not have generated more than two monophosphopeptides of a unique N-terminal sequence (in Table III, there were three phosphopeptides beginning with the sequence Q-P-D-G-P).

From the central domain, two monophosphopeptides were purified and sequenced. The coelution of these peptides by reverse-phase chromatography is an important finding of this study, and will be considered in more detail under Discussion. Of the three bisphosphopeptides analyzed, none included phospho-Tyr^{1158}, and these apparently arose by heterogeneous C-terminal tryptic cleavages (Table I). The carboxy-terminal domain phosphopeptides were obtained in the expected constellation of mono- and bisphosphopeptides, although there was evidence for unusual cleavages.

This study allows us to interpret the [^{32}P]phosphopeptide maps obtained from reverse-phase HPLC, to correlate each phosphopeptide "peak" with specific autophosphorylation sites, and to show that these phosphopeptides generally elute in clusters associated with their domains of origin (Figure 4). The phosphopeptide map obtained from autophosphorylated 38-kDa CKD (Figure 4B) confirmed that the carboxy-terminal [^{32}P]phosphopeptides elute in the range 47–66 min; the controlled cleavage of native 48-kDa CKD has been reported by others to remove the two carboxy-terminal autophosphorylation sites (Levine & Ellis, 1991; Herrera et al., 1988). The general order of [^{32}P]phosphopeptide elution is consistent with the amino acid sequence and stoichiometry of phosphorylation of each peptide.

DISCUSSION

This study was undertaken after we observed that the tryptic [^{32}P]phosphopeptide maps were dramatically different at different ATP concentrations, as reported in the preceding paper (Kohanski, 1993). In order to interpret those maps, it was necessary to identify the autophosphorylation sites included in each [^{32}P]phosphopeptide. By taking advantage of the quantities of cytoplasmic kinase domain that can be purified, we were able to isolate picomole quantities of the [^{32}P]phosphopeptides. In turn, this permitted the chemical identification of unreacted tyrosyl residues during the sequence analysis. The specific radioactivity of each phosphopeptide was determined from the sequence analysis data, yielding stoichiometries of phosphorylation for most peptides. These two facts were used to establish the locations of phosphotyrosyl residues. This allowed us to demonstrate the two juxtamembrane autophosphorylation sites at Tyr^{965} and Tyr^{972}, that Tyr^{1158} was the least phosphorylated residue in the central region, and to analyze a total of 19 discrete purified [^{32}P]phosphopeptides.

In contrast to other reports (Herrera & Rosen, 1986; White et al., 1988; Flores-Riveros et al., 1989; Tornqvist et al., 1987;

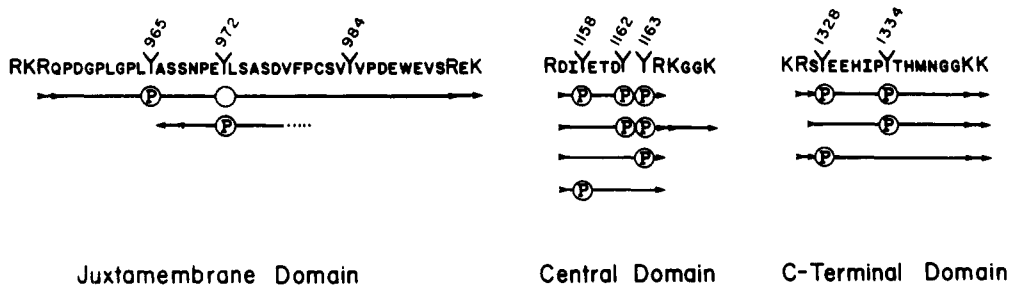

FIGURE 3: [^{32}P]Phosphopeptides of the insulin receptor. This scheme summarizes the number of phosphorylation sites on each tryptic [^{32}P]phosphopeptide of the human insulin receptor. The phosphorylation of each tyrosyl group is indicated by the P in a circle below the respective tyrosine; the open circle indicates that there may have been a bisphosphopeptide including Tyr^{972}. Amino acid sequences are given in the single-letter code; each tyrosyl group is numbered according to Ebina (1985). The tryptic cleavages that are known or inferred are indicated by the arrowheads pointing to the right. The abnormal cleavage sites, not expected from tryptic digestion, are indicated by the arrowheads pointing to the left. Further details are given in the text.

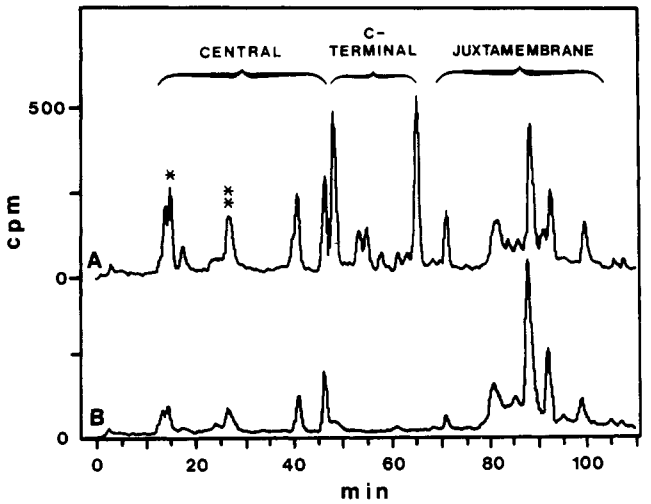

FIGURE 4: Tryptic [^{32}P]phosphopeptide maps and autophosphorylation domain assignments. The autophosphorylation reactions were done for 60 min at 100 μM [γ-^{32}P]ATP and 5 mM $Mn(CH_3CO_2)_2$, with 0.25 μM 48-kDa CKD (profile A) or 0.15 μM 38-kDa CKD (Profile B), as described in the text. Isolation and tryptic digestion of the ^{32}P-labeled CKDs and conditions for reverse-phase HPLC are described under Experimental Procedures. Under these chromatographic conditions, the [^{32}P]phosphopeptides elute in the order central domain, 12–46 min; C-terminal domain, 47–66 min; and juxtamembrane (N-terminal domain), 70–105 min. The exceptions are indicated by a single asterisk (*) for phosphopeptide I-1 and by a double asterisk (**) for phosphopetide G-1, which originate from the juxtamembrane and carboxy-terminal domains, respectively. The 38-kDa CKD, with an intact amino terminus but lacking the carboxy-terminal ≈10 kDa, lacks the C-terminal autophosphorylation sites.

Tavare & Denton, 1988), we show that bisphosphopeptides from the central domain included phospho-Tyr^{1162} and phospho-Tyr^{1163}, but not phospho-Tyr^{1158}. The two monophosphopeptides that coeluted by reverse-phase HPLC were separable by anion exchange chromatography. If these peptides were not separated and radiochemical sequence analysis alone was employed, it would have appeared that a single bisphosphopeptide was present. However, the unreacted Tyr^{1158} was identified chemically and unambiguously in four of six sequence analyses of central domain phosphopeptides (Table I). These results show conclusively that Tyr^{1158} is *not* the obligatory first autophosphorylation event, as suggested by White et al. (1988).

We have shown that some phosphopeptides resulted from anomalous cleavage of the autophosphorylated protein. This result is important since most reports on the identification of autophosphorylation sites have assumed correct tryptic cleavage; i.e., solely at Arg or Lys. In fact, our own initial work showed that most of the [^{32}P]phosphopeptide maps previously published from this laboratory, although reproducible over a period of three years, were the result of predominantly artifactual cleavages, mixed with proper tryptic cleavages. We had purified and sequenced three major phosphopeptides from conditions used to generate those maps and found phosphopeptides with sequences Asp-Tyr-PTyr-Arg (abnormal cleavage at Thr^{1160}; retention time of 28 min) and Ile-Pro-PTyr-Thr-His plus Ser-PTyr-Glu-Glu-His (abnormal cleavage at His^{1331}; retention times of 32 and 16 min, respectively); the gradients used in those studies for the reverse phase maps were different from those reported here [see Figure 7 in Kohanski and Schenker (1991)]. These abnormal cleavages appeared to result from the conditions used for SDS–PAGE. Allowing the cast gels to stand for at least 24 h, using deionized acrylamide, and employing low voltage for the electrophoresis seemed to reduce these artifactual cleavages significantly, as shown by the sequence analyses reported here.

There are other significant differences between our results and those of other laboratories (Herrera & Rosen, 1986; White et al., 1988; Flores Riveros et al., 1989; Tornqvist et al., 1987; Tavare & Denton, 1988). The first report of the domains undergoing autophosphorylation was by Herrera and Rosen (1986). That study used antipeptide antibodies directed against selected potential autophosphorylation regions and was conclusive regarding two of the three domains where autophosphorylation occurs. Radiochemical sequence analysis was employed in three of the studies: The data presented by Tornqvist and Avruch (1987) showed a significant lag in the recovery [^{32}P]PTH-phosphotyrosine, even during solid-phase sequence analysis. Coupled with direct chemical sequence analysis, they could be certain of the domain assignment of each of five [^{32}P]phosphopeptides and in general of the individual residues phosphorylated. In the report by Flores-Riveros et al. (1989; see Figure 13), radiochemical sequence analysis revealed a substantial lag in the recovery of ^{32}P as far as seven cycles after the presumed carboxy terminus of the phosphopeptide had been reached. They also reported that in total ≈10% of the applied radioactivity was recovered in the fractions in each sequence analysis. Because of these low yields, fluctuations in cycle-to-cycle recovery of [^{32}P]PTH-phosphotyrosine are potentially misleading. Importantly, however, they provided direct evidence for carboxy-terminal heterogeneity in two of the phosphopeptides. Here we have been able to add direct evidence for amino-terminal heterogeneity of certain peptides as well. Similar problems of amino- and carboxy-terminal heterogeneity, as well as the lag in recovery of ^{32}P, were evident in the study by White et al. (1988), coupled with the fact that only a single separation method was used prior to radiochemical sequence analysis. From the data in Table I and the elution profiles in Figure

2 (this report), it can be seen that several [^{32}P]phosphopeptides coelute during reverse-phase HPLC separation. Coelution would certainly present substantial problems in the identification of which residues in the sequence are autophosphorylated and may explain why they failed to identify these monophosphopeptides from the central domain.

The two-dimensional mapping protocol used by Tavare and Denton (1988) assigned the autophosphorylation sites of each [^{32}P]phosphopeptide according to electrophoretic mobilities and subdigestions with endoproteinase Glu-C (V8 protease). They assigned two phosphopeptides, B2 and B3, to the central domain and concluded that these represented bisphosphopeptides including phospho-Tyr^{1158} and either phospho-Tyr^{1162} or phospho-Tyr^{1163}. However, employing the same mapping procedure but using a mutant with Tyr^{1158} changed to Phe, these same two phosphopeptides were observed (Zhang et al., 1991). The data shown here (Table I) demonstrate that Tyr^{1158} is not abundantly autophosphorylated, and the major bisphosphopeptides of the central domain include only phospho-Tyr^{1162} and phospho-Tyr^{1163} and not phosphorylation of Tyr^{1158}. These findings are consistent with the observations of Zhang et al. (1991). We therefore believe that the alleged activating role of Tyr^{1158} (White et al., 1988) should be reconsidered.

Identification of the two autophosphorylation sites in the juxtamembrane domain (the amino-terminal domain of the CKD) has not been reported. However, all groups have reported that the phosphopeptides not identified in their analyses were large and hydrophobic. These observations are consistent with the elution positions of the juxtamembrane domain phosphopeptides at the end of the gradient under reverse-phase HPLC conditions, shown in Figures 2 and 4, and as noted previously by White et al., (1988). We have identified Tyr^{965} and Tyr^{972} as autophosphorylation sites. There are reports concerned with the functional roles of the juxtamembrane region (Thies et al., 1990; Rajagopalan et al., 1991; White et al., 1988b), which naturally raise questions regarding autophosphorylation in this subdomain. The mapping and identification of two tyrosine residues phosphorylated in the juxtamembrane region may help to further clarify our understanding of the functions served by this domain.

ACKNOWLEDGMENT

The author thanks Yuan-Ping Han for purification of the cytoplasmic kinase domain and Dr. Esther Schenker for [γ-^{32}P]ATP synthesis.

REFERENCES

Biener, Y., & Zick, Y. (1990) *Eur. J. Biochem. 194*, 243.
Ebina, Y., Ellis, L., Jarnagin, K., Edery, M., Graf, L., Clauser, E., Ou, J., Masiarz, F., Kan, Y. W., Goldfine, I. D., Roth, R. A., & Rutter, W. J. (1985) *Cell 40*, 747.
Flores-Riveros, J. R., Sibley, E., Kastelic, T., & Lane, M. D. (1989) *J. Biol. Chem. 264*, 21557.
Fujita-Yamaguchi, Y., Sacks, D. B., McDonald, J. M., Sahal, D., & Kathuria, S. (1989) *Biochem. J. 263*, 813.
Herrera, R., & Rosen, O. M. (1986) *J. Biol. Chem. 261*, 11980.
Herrera, R., Lebwohl, D., Garcia de Herreros, A., Kallen, R. G., & Rosen, O. M. (1988) *J. Biol. Chem. 263*, 5560.
Kasuga, M., Fujita-Yamaguchi, Y., Blithe, D. L., & Kahn, C. R. (1983a) *Proc. Natl. Acad. Sci. U.S.A. 80*, 2137.
Kasuga, M., Fujita-Yamaguchi, Y., Blithe, D. L., White, M. F., & Kahn, C. R. (1983b) *J. Biol. Chem. 258*, 10973.
Kohanski, R. A. (1989) *J. Biol. Chem. 264*, 20984.
Kohanski, R. A. (1993) *Biochemistry* (preceding paper in this issue).
Kohanski, R. A., & Schenker, E. (1991) *Biochemistry 30*, 2406.
Laemmli, U. K. (1970) *Nature 227*, 680.
Levine, B. A., & Ellis, L. (1991) *J. Biol. Chem. 266*, 12369.
Morrison, B. D., Feltz, S. M., & Pessin, J. E. (1989) *J. Biol. Chem. 264*, 9994.
Palmer, J. L., & Avruch, J. (1981) *Anal. Biochem. 116*, 372.
Rajagopalan, M., Neidigh, J. L., & McClain, D. A. (1991) *J. Biol. Chem. 266*, 23068.
Sacks, D. B., & McDonald, J. M. (1988) *J. Biol. Chem. 263*, 2377.
Tavare, J. M., & Denton, R. M. (1988) *Biochem. J. 252*, 607.
Tavare, J. M., Clack, B., & Ellis, L. (1991) *J. Biol. Chem. 266*, 1390.
Thies, R. S., Webster, N. J., & McClain, D. A. (1990) *J. Biol. Chem. 265*, 10132.
Tornqvist, H. E., Pierce, M. W., Frackelton, A. R., Nemenoff, R. A., & Avruch, J. (1987) *J. Biol. Chem. 262*, 10212.
Villalba, M., Wente, S. R., Russell, D. S., Ahn, J. C., Reichelderfer, C. F., & Rosen, O. M. (1989) *Proc. Natl. Acad. Sci. U.S.A. 86*, 7848.
Walseth, T. F., & Johnson, R. A. (1979) *Biochim. Biophys. Acta 562*, 11.
White, M. F., Shoelson, S. E., Keutmann, H., & Kahn, C. R. (1988a) *J. Biol. Chem. 263*, 2969.
White, M. F., Livingston, J. N., Backer, J. M., Lauris, V., Dull, T. J., Ullrich, A., & Kahn, C. R. (1988b) *Cell 54*, 641.
Zhang, B., Tavare, J. M., Ellis, L., & Roth, R. A. (1991) *J. Biol. Chem. 266*, 990.